An Artificial Neural Network Emulator of the Rangeland Hydrology and Erosion Model

Mahmoud Saeedimoghaddam[1], Grey Nearing[2], Mariano Hernandez[3], Mark A. Nearing[3], David C. Goodrich[3], Loretta J. Metz[4]

[1]Department of Land, Air & Water Resources, University of California, Davis, CA, USA
[2]Google Research, Mountain View, CA, USA
[3]USDA-Agricultural Research Service, Southwest Watershed Research Center, Tucson, AZ, USA
[4]USDA-NRCS Resource Inventory and Assessment Division, CEAP-Grazing Lands, Tucson, AZ, USA

Key Points:

- We designed an artificial neural network that is able to recreate the outputs of the RHEM.
- The network is 13 billion times faster than the RHEM which is critical when numerous runs are needed.
- We evaluated the network with multiple approaches to ensure that it recreates the RHEM accurately.

Abstract

Machine learning (ML) is becoming an ever more important tool in hydrologic modeling. Many studies have shown the higher prediction accuracy of the ML models over traditional process-based ones. However, there is another advantage of ML which is its lower computer time of execution. This is important for the applications such as hydraulic soil erosion estimation over a large area and at a finer spatial scale. Using traditional models like Rangeland Hydrology and Erosion Model (RHEM) requires too much computation time and resources. In this study, we designed an Artificial Neural Network that is able to recreate the RHEM outputs (runoff, soil loss, and sediment yield) with high accuracy (Nash-Sutcliffe Efficiency ≈ 1.0) and a very low computational time (13 billion times faster on average). We ran the RHEM for more than a million synthetic scenarios and train the Emulator with them. We also, fine-tuned the trained Emulator with the RHEM runs of the real-world scenarios (more than 32,000) so the Emulator remains comprehensive while it works specifically accurately for the real-world cases. We also showed that the sensitivity of the Emulator to the input variables is similar to the RHEM and it can effectively capture the changes in the RHEM outputs when an input variable varies. Finally, the dynamic prediction behavior of the Emulator is statistically similar to the RHEM with a 95% confidence interval.

1 Introduction

Machine learning (ML) is becoming an increasingly important tool for hydrologic modeling (Lange & Sippel, 2020; Sit et al., 2020). There are three main reasons why ML can be advantageous for hydrologic (and other types of) applications. First, relative to process-based and even conceptual models, ML models are inexpensive to train (calibrate) and run – often requiring orders of magnitude less computational expense. Second, ML models are often significantly more accurate than physics-based models in certain hydrological applications (Hsu et al., 2002; Nearing et al., 2018; Kratzert et al., 2019), due

Corresponding author: Mahmoud Saeedimoghaddam, msaeedi@ucdavis.edu

to the fact that many components of hydrological theory are not valid at scales that are relevant to real-world applications (Dooge, 1986; Nearing et al., 2021). Third, ML models allow for extracting information from different types of predictor (input) variables, because these models are not constrained by a need for explicit, prescribed (e.g., biogeophysical) relationships between the model inputs and targets.

In this paper, we develop, train, and test a ML-based soil erosion model motivated by the first and third reasons listed above. As an example of the type of problem that motivates this effort, the Daily Erosion Project (`https://www.dailyerosion.org/`) (Gelder et al., 2018) uses the Watershed Erosion Prediction Project (WEPP) model (A. Nearing et al., 1989) and other tools to estimate daily soil erosion and surface water runoff on hill slopes in Iowa based on the previous day's weather estimated from satellite data (Cruse et al., 2006). Results from this tool are useful for conservationists and land managers, however scaling such an application to larger areas, longer time periods, or finer spatial resolutions would require significant investment in compute time and resources. Another example is the Rangeland Hydrology and Erosion Model (RHEM), which is a process-based hydraulic soil erosion prediction tool specific for rangeland application (Hernandez et al., 2017). RHEM predicts runoff, soil loss, and sediment yield of storm events with sufficient accuracy for a wide range of applications in rangeland systems. (A. Weltz et al., 2014) executed RHEM for more than 10,000 sites using ground-measured, National Resources Inventory (NRI) data for the western United States, which required many days of computer time. Such computational expense precludes large-scale runs in real time, and also limits large scale ensemble runs. Additionally, it is not feasible to conduct ground surveys to estimate the required RHEM input parameters (e.g., ground cover) on all rangelands in the United States. Having a pre-trained ML-based erosion model will allow for learning directly from different types of (e.g., remote sensing) input data, which is necessary to produce model-based erosion or erodibility estimates outside of ground survey locations. In this paper we do not report results from using remote sensing data (those results are described in a separate paper), however the first step in doing that is to build, train, and verify a ML erosion model that can serve as a base model for future studies.

Our objective is to create and train an artificial neural network that provides a solid foundation for application-specific work with ML-based rangeland soil erosion modeling. The proposed neural network emulates the RHEM. We demonstrate that this emulator accurately reproduces the RHEM outputs over a wide range of input parameters, with several orders of magnitude less computation time. We test the reliability of this emulator through multiple analyses – i.e., to understand whether the emulator responds similarly to the RHEM with changes to individual inputs. To be clear, we are *not* developing a ML model with the goal of achieving higher accuracy than the RHEM (i.e., the second of three common advantages of ML models listed in the first paragraph of this section). This is because we do not have the large amount of measured erosion data that would be necessary to train an observation-based model directly. As an example, Interagency Rangeland Water Erosion Team measured the runoff, and sediment discharge on 204 plots from 49 rangeland sites in the United States of America (Wei et al., 2009) which is a relatively small data size. These datasets could be leveraged to build more accurate data-driven erosion models, however the techniques for doing this – e.g., few-shot learning (Wang et al., 2020), transfer learning (Zhuang et al., 2021), or fine-tuning (Vrbančič & Podgorelec, 2020) – generally require a *base model*. A base model is a deep learning model that is pre-trained on a large dataset, that can then be tuned or adjusted using smaller datasets (Tajbakhsh et al., 2016). This is the third objective for the the emulator that we develop in this paper – as a base model for few-shot learning. The model, along with our training pipeline, all of the Python scripts we used for the cross validation and the sensitivity analysis, and our model's pre-trained weights are open source and publicly available at the GitHub link in the Code and Data Availability section below. Anyone is welcome to use this model directly, or as a base model for further ML research in this topic area.

2 Materials and Methods

In this section we start by providing a brief explanation of RHEM, including its inputs, parameters, and outputs. For a more comprehensive description of RHEM, see Al-Hamdan et al. (2015) and Hernandez et al. (2017). After that, we explain the architecture of our neural network Emulator of RHEM in detail. Finally, we describe methods used for analyzing the accuracy of the Emulator and the sensitivity of both models to inputs and changes in inputs, which will be used to demonstrate that the Emulator has similar behavior and functionality to RHEM.

2.1 The RHEM

The RHEM (Version 2.4) consists of two sets of equations (Hernandez et al., 2017): first, overland flow equations, in which, the flow per unit width across a plane surface at any time is calculated by a partial differential equation (PDE) (Equation (1)):

$$\frac{\partial h}{\partial t} + \frac{\partial q}{\partial x} = \sigma(x,t), \tag{1}$$

where h is the flow depth at time t and the position x, q is the volumetric water flux per unit plane width, and σ is the rainfall excess. Solving Equation (1) for the entire plane during a rainfall event results in the surface runoff (mm). Runoff is one of the three outputs of the RHEM.

The second set of equations describe overland soil erosion, deposition, and transport by modeling the movement of suspended sediment in a concentrated flow area:

$$\frac{\partial (Ch)}{\partial t} + \frac{\partial (Cq_r)}{\partial x} = D_{ss} + D_{cf}, \tag{2}$$

where C is the measured sediment concentration, q_r is the flow discharge of concentrated flow per unit width, D_{ss} is the splash and sheet detachment rate, and D_{cf} is the concentrated flow detachment rate. Solving Equation (2) during a rainfall event for the entire plane results in soil loss ($\frac{ton}{ha}$) and for the ending point of the plane results in sediment yield ($\frac{ton}{ha}$) which are the other two outputs of the RHEM.

The required parameters to solve Equations (1) and (2) are estimated by the four groups of the user inputs related to: storm event(s), slope, soil, and cover (see Figure 1 of Al-Hamdan et al. (2015)). Table (1) shows the RHEM input parameters (center and right-hand columns) and their relationship to user inputs on the USDA RHEM web application tool (`apps.tucson.ars.ag.gov/rhem`; left-hand column). For Equation 1, K_e and F_t are required to estimate the infiltration rate (f) and q respectively. For Equation 2, K_{ss} is required to estimate Dss. Some of the parameters in the RHEM physics are not mentioned in Table (1) because RHEM web application tool considers them hard-coded constants. One of these is stream power erodibility (K_ω =0.0000077470 $\frac{s^2}{m^2}$) used to estimate D_{cf} in Equation 2. The rest of these hard coded parameters are Slope length (L=50m), Slope width (Width=1m), Coefficient of variation for effective hydraulic conductivity (CV=1), Initial degree of soil saturation (SAT=0.25), Maximum concentrated erodibility (K_{cm} = 0.000299 $\frac{s^2}{m^2}$), Cover fraction of surface covered by intercepting cover (CA=1), Interception depth (IN=0m), Volumetric rock fraction (Rock=0), variable α in the infiltration Smith-Parlange Equation (ALF=0.8), Rill spacing (RSP=1m), Average micro topographic spacing (Spacing=1m), Fraction of bare soil to total area (Bare=0), and β decay factor in the detachment equation (ADF=0 $\frac{1}{m^2}$). The Bare and β are equal to zero meaning that they are inactive. They are going to be activated in the future to test the RHEM for disturbed conditions.

To estimate general erodibility in a given location, RHEM is typically run many times over many synthetic storm events, and the results are aggregated to annual mean values (the USDA RHEM web tool uses the CLImate GENerator (CLIGEN) model (Lane & Nearing, 1989) to generate synthetic daily storm events in a specific region.). For example, runoff, soil loss, and sediment yield outputs of the RHEM tool are reported as the annual mean values over 300 years (A. Weltz et al., 2014). This is computationally expensive but necessary given that RHEM simulates physical processes at the event scale. In this study, instead of emulating the actual event-based model, we design a neural network which is able to directly estimate the aggregated output values.

Table 1. RHEM input parameters and their relations to the user inputs to the RHEM web application (`apps.tucson.ars.ag.gov/rhem`). e.g. calculation of K_e needs soil texture, foliar and ground cover.

User Inputs to the RHEM Web Application	Input Parameters to the RHEM Physics Module	Abbreviation
Storm		
CLIGEN[a] *Station*	Rainfall Volume(mm)	prcp
	Rainfall Duration(h)	dur
	Rainfall Peak intensity	tp, ip
Slope		
Steepness%	Slope steepness%	slp
	Friction factor	F_t
Shape	Slope Shape	slpshp
Soil		
Texture	Mean capillary drive (mm)	G
	Pore size distribution	dist
	Porosity	por
	Upper limit to saturation	smax
	Particle class fractions	frac 1-5[b]
	Effective hydraulic conductivity	K_e
FoliarCover%		
(*BunchGrass*, *Forbs*,	Effective hydraulic conductivity	K_e
Shrubs, *SodGrass*)	Splash and Sheet erosion	K_{ss}
GroundCover%		
(*BasalPlant*,	Friction factor	F_t
Rock, *Litter*	Effective hydraulic conductivity	K_e
BiologicalCrusts)	Splash and Sheet erosion	K_{ss}

[a] CLIGEN: stochastic weather generator model

[b] frac1: Clay, frac2: Silt, frac3: small aggregates, frac4: large aggregates, frac5: Sand

2.2 The RHEM Emulator

Inputs to the Emulator consist of 25 variables listed in Table (2). The climatic inputs are from the CLIGEN stations. However, the Emulator uses the average prcp, dur, tp and ip over 300 years. The slope and the soil inputs are the same as input parameters to the RHEM physics module. RHEM uses Foliar and Ground cover values to cal-

culate its input parameters like K_{ss} (Table (1)). The Emulator bypasses these calculations and uses the Foliar and Ground covers directly as its input variables.

Table 2. The Emulator inputs and their sources

Emulator Inputs	Abbreviation	Source
Rainfall Volume(mm)	prcp	
Rainfall Duration(h)	dur	
Rainfall Peak intensity	tp, ip	
Slope steepness%	slp	
Slope Shape	slpshp	Input Parameters to
Mean capillary drive	G	the RHEM Physics Module
Pore size distribution	dist	
Porosity	por	
Upper limit to saturation	smax	
Particle class fractions	frac 1-5	
Total foliar cover%		
Bunch Grass%		
Forbs%		
Shrubs%		
Sod Grass%		User Inputs to
Total ground cover%		the RHEM Web Application
Basal Plant%		
Rock%		
Litter%		
Biological Crust%		

Figure (1) shows the structure of our neural network RHEM Emulator (left panel), and compares this with the structure of RHEM (right panel). Part A of the models is responsible for calculating runoff and part B determines soil loss and sediment yield. The "n events" notation on the right panel refers to the fact that, the RHEM computes the outputs for individual (synthetic) storm events (e.g., daily over 300 years) and reports the average values. The Emulator on the other hand, directly calculates average values for runoff, soil loss, and sediment yield.

Inputs to the Emulator are fed into a Fully Connected (FC) layer of size 256 with Parametric Rectified Linear Unit (PReLU) activation functions (He et al., 2015). PReLU helps the gradient descent algorithm to bypass the local minimums of the cost function. The output of the first FC layer is shared between parts A and B of the model (runoff and sediment processes, respectively), which means that this input layer contains all the basic information for estimating the runoff, soil loss and sediment yield. Thirty-nine Parameters of the RHEM (Table 2), on the other hand, are used for estimating q, f, D_{ss}, D_{cf} and eventually solving Equations (1) and (2) as described in Section 2.1.

Part A of the Emulator (runoff) starts with five successive FC layers (PReLU activation) of size 256 followed by another FC layer (PReLU activation) of size 16. after each one of those FC layers we applied a Batch Normalization (BN) layer (Ioffe & Szegedy, 2015). By maintaining the mean of the layer's output close to 0 and the standard deviation close to 1, BN layer not only increases the training speed but also induces a more predictive and stable behavior of the gradient (Santurkar et al., 2018). The output of

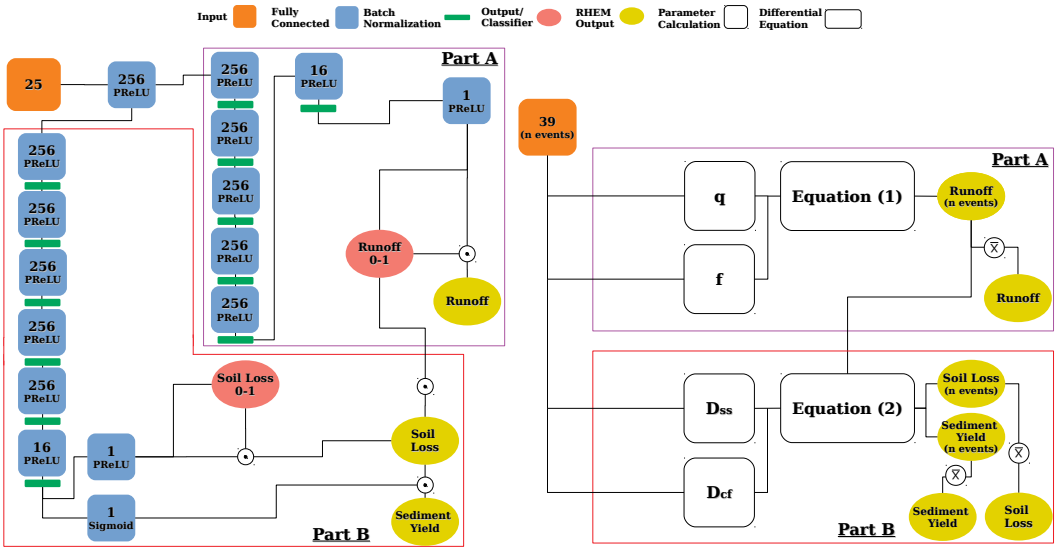

Figure 1. The Emulator architecture (Left panel) along with its RHEM counterpart (Right panel). $\odot$ is the matrix element-wise multiplication symbol and the circled $\bar{x}$ is the average function over 300 years. Thirty-nine input variables of the RHEM includes those listed in Table (1) and the hard-coded ones explained in section 2.1. The "n events" notation on the right panel refers to the fact that the RHEM calculations are based on the individual storm events.

the last BN layer is then fed into another FC layer (PReLU activation) of size 1 which calculates the final runoff value. To ensure that the model produces zeros for the cases that the runoff is roughly zero, a binarization function is applied to the estimated runoff (0 if runoff=0 and 1 otherwise) and compared to the binarized runoff of the training dataset. The binarized values are then multiplied (element-wise multiplication) by the estimated runoffs which results in the final runoff outputs of the Emulator.

In part B, the shared FC layer of the Emulator (the first 256-neuron layer, shared between parts A and B of the Emulator) is fed into a set of five FC layers (PReLU activation) of size 256 followed by another FC layer (PReLU activation) of size 16. Same as part A, we applied the BN layers on each layer's output. The final BN layer is first fed into the FC layer (PReLU activation) of size 1 to estimate the soil loss output. This output is modified in two ways. First, similar to how runoff is treated, a binarization function is applied to the estimated soil loss to ensure that the model generates zeros for the cases that the soil loss is roughly zero (0 if soil loss=0 and 1 otherwise) and compared to the binarized soil loss of the training dataset. These binarized values are then multiplied (element-wise multiplication) by the estimated soil losses. Second, to ensure that soil loss is zero if there is no runoff, the soil loss values are multiplied (element-wise multiplication) by the binarized runoffs from part A. These two modifications generate the final soil loss output of the Emulator that are constrained to physically realistic values. As the value of sediment yield is a portion of the soil loss, the output of the final BN layer is fed into the FC layer (Sigmoid activation) of size 1 and the result is then multiplied (element-wise multiplication) by the soil loss which results in the final sediment yield output of the Emulator.

The number of FC layers and also their activation functions have been selected by several manual trials. The sizes of the FC layers on the other hand have been tuned using a process described in Appendix A. Overall, the Emulator has 678,277 trainable parameters.

2.3 Model Accuracy Analysis

In this study we report three metrics suggested by (Gupta et al., 2009) to assess the Emulator performance:

1- Nash-Sutcliffe Efficiency (NSE) which is equivalent to coefficient of determination (R^2):

$$NSE = 1 - \frac{\frac{1}{N}\sum_{n=1}^{N}(o_n - e_n)^2}{\sigma_o^2} \tag{3}$$

where o is the observed value of the output, e is the Emulator estimation of the output, N is the data size and, σ_o^2 is the variance of the observed values.

2- α-NSE decomposition which measures the relative variability in the estimated and observed values:

$$\alpha = \frac{\sigma_s}{\sigma_o} \tag{4}$$

where σ_s is the standard deviation of the Emulator estimation of the output and σ_o is the standard deviation of the observed output values.

3- β-NSE decomposition which captures the normalized bias in the Emulator estimation:

$$\beta = \frac{\mu_s - \mu_o}{\sigma_o} \tag{5}$$

where μ_s is the average of the model estimation values and μ_o is the average of the observed values.

We used these metrics over the 10 fold cross validation experiments (90% of the data or 931,797 samples for training and 10% or 103,533 samples for the test) and also over the model testing with a real world dataset which is described in section 3.

2.4 Sensitivity Analysis

Our objective is for the Emulator to not only match RHEM outputs in cross-validation, but also to ensure that the Emulator responds in physically realistic ways to changing inputs. We did this using local and global sensitivity analysis.

Global sensitivity analysis (GSA) allows us to compare the average responses of RHEM and the Emulator to each input variable. GSA calculates the overall effect of a parameter on a model over the entire parameter space. In this study, we used a variance-based method named Random Balance Designs Fourier Amplitude Sensitivity Test (RBD-FAST) (Tarantola et al., 2006): This method is a combination of Satterthwaite's Random Balance Designs (RBD) (Satterthwaite, 1959) with the Fourier Amplitude Sensitivity Test (FAST) (Cukier et al., 1973). Variance-based methods decomposes the variance of the model output into partial variances contributed by different model parameters. The main or first order effect of parameter X_i measures the effect of varying X_i only:

$$S_i = \frac{V_{Xi}(E_{X\sim i}(Y|X_i))}{V(Y)} \tag{6}$$

where S_i is the first order effect X_i, $X_{\sim i}$ is the matrix of all factors but X_i and Y is the model output. The inner expectation of the denominator is the mean of the model outputs when X_i is fixed and the outer variance is for all possible $X-i$ values (Saltelli et al., 2010). FAST method introduces a signal for each parameter using a periodic sampling approach and a Fourier transformation to decompose the variance (Xu & Gertner,

2011) and to create the nominator of Equation (6). To reduce the complexity and computational cost of FAST, its periodic sampling procedure has been modified by an RBD approach (Tarantola et al., 2006).

In this study, we used SALib package of Python programming language (Herman & Usher, 2017) to implement the sensitivity analyses.

2.5 Change in the Model Prediction by Altering the Variables

Although the GSA visualizes the effects of the variables on both models, it does not show the change pattern of the outputs by altering the input variables. We defined a set of scenarios in which all of the variables are fixed except for the one that increases. To generate the scenarios, first we defined a benchmark (Table 3) in a way that the scenarios produce a vast range of the outputs that covers a larger portion of the output space. Then, by increasing a specific variable, while keeping the others fixed, we made a set of scenarios for that variable. There were some restrictions in defining the scenarios for some variables: 1- The Ground cover categories could be increased as far as they sum up to 100%. Complying with this rule, we created 43 scenarios for each one of the Litter, Biological Crusts, Rock and Basal covers. Same rule should be followed for Foliar cover and as a result we generated 43 scenarios for Bunch Grass, Forbs, Shrubs and Sod Grass. 2- The four variables of the CLIGEN stations (prcp, dur, tp, ip) should increase at the same time. Following this rule, we were able to capture 7 stations. Finally, for the slope shape we made 3 scenarios (including the benchmark) and for the slope steepness we made 50 scenarios. We ran the RHEM and the Emulator for those scenarios to depict the change patterns of the model outputs.

Table 3. The benchmark scenario

Litter	Biological Crusts	Basal	Rock	Forbs	Bunch Grass	Shrubs	Sod Grass	Soil	Slope	Slope Shape	CLIGEN
5%	5%	5%	5%	5%	5%	5%	5%	Clay	50%	Uniform	481570

2.6 Compare the Dynamic Prediction Behaviors of the Models

Any changes even a small one in the components of a landscape could result in a significant alteration in the erosion pattern of that landscape. The Emulator should be able to capture those changes in the same way as the RHEM. Thus, it is important to know if the difference between the outputs of the Emulator in time $t1$ and $t2$ for a specific location is statistically equal to the difference of the RHEM outputs. While in other sections we used the whole NRI dataset, in this specific analysis, we only used the NRI points which 1- have been surveyed more than once, 2- the difference between their last and their first survey dates were greater than or equal to five years and, 3- the surveys were in the same season. The total number of NRI points after the aforementioned filters is 2,402. For each location we calculated the difference between the RHEM runoff values of the two dates. We calculated the same thing for the Emulator runoff values. Including the soil loss and the sediment yield to the process, we ended up with 6 difference values for each location. To compare the dynamic prediction behaviors of the models, we performed an independent samples t test to statistically compare the mean values of the differences (Null hypothesis: Equal means). We also implemented a Pearson's r correlation test between the differences to statistically compare the directions of their changes (Null hypothesis: No linear relationship). Furthermore, we implemented the tests for multiple ranges of the differences for more detailed examinations.

2.7 Model Training

The most important goal of the Emulator is to predict the outputs as close as possible to the RHEM in the real world scenarios. Thus, one may collect the real world scenarios from different sources such as NRI dataset to train the Emulator. However, those sources may not contain enough data as Neural Networks need to be trained with large datasets for a good performance (Sun et al., 2017); also, the range of the input variables in real world data does not cover the whole variable space and training only with those data may not result in a comprehensive model. Thus, we trained the Emulator with a large synthetic dataset that covers the entire variable space (Section 3). Emulator was trained for 300 epochs with an Adam optimizer (Kingma & Ba, 2014). Equation (7) shows the learning rate decay function utilized by the optimizer:

$$LR_{epoch} = LR_i \times a^{\lfloor \frac{epoch}{b} \rfloor} \tag{7}$$

where LR_{epoch} is the learning rate at each epoch. LR_i is the initial learning rate, a is a parameter that controls the decay rate, and b is the number of epochs before a decrease.

Using the hyperparameter tuning process described in Appendix A, we chose 0.001, 0.5, 50, 1000 for initial learning rate and parameters a and b of the decay function and the batch size respectively.

The loss function was constructed as a combination of losses over the three RHEM outputs variables: runoff, soil loss, and sediment yield. A weighted binary cross entropy (Aurelio et al., 2019) loss was used for the runoff and soil loss binary classifiers (to train the part of the model that allows for zero-valued outputs and ensures that the soil loss is zero if there is no runoff), and mean squared error (MSE) was used for the runoff, soil loss and sediment yield regressions. Input variables were individually scaled to [0, 1], and since the distributions over outputs are heavy-tailed, we transformed outputs logarithmically and then scaled to [0, 1] for training. All evaluation metrics are reported on the non-transformed, unscaled output data.

As was mentioned before, the accuracy of the Emulator is specifically important for the real world scenarios. No sampling methods guarantee to produce enough samples within the variable range of the real world scenarios. In order to increase the precision of the trained Emulator for those cases while keeping it comprehensive, we fine tuned the trained Emulator with the real world scenarios. Fine tuning means retraining the Emulator by the additional scenarios and slightly adjust its weights and biases with a small learning rate (Renda et al., 2020). Here, we retrained the Emulator using NRI dataset described in Section 3 (epoch=100, batch size=1,000). For the learning rate decay function, we used Equation (7) with 3.125×10^{-5}, 0.5 and 50 as the initial learning rate, parameters a and b respectively ($3.125 \times 10^{-}5$ is the last learning rate used in the Emulator training phase.).

Finally, while the original RHEM has been programmed by FORTRAN language, In this study, the Emulator and all analyses were implemented in Python. The Emulator was developed as a Keras module using Tensorflow2 (Abadi et al., 2015).

3 Data

In this study, we used Latin hypercube sampling method (Mckay et al., 2000) to create 1 million synthetic RHEM scenarios from the n-dimensional input space, where n=25 is the number of input variables. For making a uniform sample of size N=1e6 that covers the entire range of the input variable space, each parameter range was partitioned into n equal-probability (n-dimensional) strata, and then a random point was drawn from

Table 4. The sample space of the one million cross-validation data points used in this study.

Model Inputs	Value Range
Storm(CLIGEN)	
prcp	[2.40, 23.23]
dur	[1.22, 14.77]
tp	[0.08, 0.30]
ip	[2.60, 5.61]
Slope	
slp(%)	[0.1,100]
slpshp	[Concave, Convex, Uniform]
Soil	
Texture	[a]12 soil texture classes
FoliarCover%	
BunchGrass	
Forbs	
Shrubs	[b][1,100]
SodGrass	
total	
GroundCover%	
BasalPlant	
Rock	
Litter	[b][1,100]
BiologicalCrusts	
total	

[a]From the US. Department of Agriculture (USDA)

[b]Four numbers between 1 and 100 which must sum to the total percentage

each stratum. Finally, the points were combined randomly to make the final sample (Mohammadi & Cremaschi, 2019). Table (4) shows the sampling range that we used for each parameter. A CLIGEN station contains a daily series of each storm parameter (prcp, dur, tp, ip) for 300 years, and since the Emulator is not an event-based model, a single value was used to represent storm parameters. We used the average value of each series and thus, a CLIGEN station is presented by four average values. Table (4) shows the range of these four averages in all 2,711 stations of the USA.

We considered concave, convex and uniform slope shapes according to NRI protocols (US Department of Agriculture, 2019). Table (5) lists the soil hydraulic parameters for all 12 texture classes used in this study. The classes are based on the U.S. Department of Agriculture (USDA) soil classification (Soil Survey Staff, 1999). Finally, for each sample, the random values of total foliar and ground cover percentages and the random combinations of their four categories were defined.

In the highly non-linear infiltration equation, when the infiltration parameters (specifically the mean capillary drive (G)) are close to their upper bounds, RHEM is unstable and may not be able to solve Equations (1) and (2). So, out of 1 million scenarios we got 998,010 successful RHEM runs, with the remainder due to RHEM failures (not the Emulator failures).

Out of 998,010 RHEM runs, 652 (0.065%) cases resulted in zero runoff and a further 54 (0.005%) cases generated zero soil loss with non zero runoff. This causes an ex-

Table 5. The values of the soil parameters for each texture class.

Soil Texture Class	por	dist	G	smax	frac1	frac2	frac3	frac4	frac5
Sand	0.3902	0.69	50	0.95	0.0077	0.018	0.0435	0.148	0.7827
Loamy Sand	0.4087	0.55	70	0.92	0.0137	0.0353	0.0951	0.233	0.6229
Sandy Loam	0.4306	0.38	130	0.91	0.0325	0.0542	0.1801	0.3939	0.3394
Loam	0.4531	0.25	110	0.94	0.0498	0.1128	0.2877	0.4004	0.1494
Silt Loam	0.4455	0.23	200	0.97	0.0505	0.3095	0.3497	0.2255	0.047
Silt	0.4258	0.23	200	0.97	0.0221	0.682	0.153	0.0916	0.0513
Sandy Clay Loam	0.4377	0.32	260	0.83	0.0641	0.0005	0.1686	0.6217	0.1451
Clay Loam	0.4589	0.24	260	0.84	0.0848	0.0397	0.3157	0.5148	0.045
Silty Clay Loam	0.4581	0.18	350	0.92	0.0861	0.1986	0.4014	0.3044	0.0096
Sandy Clay	0.4146	0.22	305	0.75	0.1073	0.0001	0.1039	0.7544	0.0344
Silty Clay	0.4704	0.15	375	0.88	0.1196	0.1517	0.3244	0.4012	0.0031
Clay	0.4724	0.16	400	0.81	0.1247	0.0001	0.2567	0.6057	0.0128

tremely imbalanced data for classifying the binarized runoff and erosion values in the Emulator. To reduce this effect, by adding random noise to the inputs parameters of the 652 and 54 runs to create more zero-ruoff and zero soil loss scenarios. Using those, we were able to append 20,749 and 16,572 additional RHEM runs with zero runoff and zero soil loss with non-zero runoff to the dataset respectively. As a result, the final size of the dataset was N=1,035,331.

For the fine tuning phase of the Emulator we used the NRI dataset (USDA, 2018). Since 2004, the USDA Natural Resources Conservation Service (NRCS) has conducted the NRI on rangelands held in non-federal ownership (privately deeded, state-owned, tribal lands, and local government-owned lands). This extensive inventory contains field-measured data for ground and foliar cover that is used as RHEM input data.

4 Results and Discussion

In this section, we present the results related to the execution time of the RHEM runs and the training and testing time of the Emulator and also, the accuracy of the Emulator for both synthetic and real (NRI) data. Then, the Sensitivity analysis of the RHEM and the Emulator are provided and compared. Moreover, the changes in the model prediction by altering each variable were demonstrated for both RHEM and the Emulator and compared. Finally, we compared the dynamic prediction behaviors of the RHEM and the Emulator.

4.1 Timing Benchmarking

We used an "Intel Xeon Silver 4110" CPU cluster with five nodes each having 40 cores to run the RHEM. Each run (over 300 years of daily CLIGEN-derived synthetic storm events) was on a single core. The average run time was 7 minute and 48 seconds. The maximum run time was 41 minutes and 2 seconds and the minimum was 12 seconds.

The Emulator ran on "NVIDIA GeForce RTX 2070 with Max-Q design" GPUs. Inference (prediction) takes a total of 3.7 seconds for all 103,533 test samples (about 0.000036 seconds per individual run). This is after training the Emulator, which is a one-time cost of 23 minutes (any future user of the Emulator will not have to train their own model – our pre-trained model is available at the GitHub repository linked in the Code and Data Availability Section).

4.2 Training Loss

Figure (2) shows the graphs of the training loss (training over the entire synthetic dataset). The soil loss classification graph starts from a higher value than the runoff classification and ends on a higher value as well (about -1 in the log scale). A possible reason could be the fact that the binary soil loss dataset is more imbalanced as we have fewer zero soil loss cases with non-zero runoff. Plots of the regression components of the loss function show that the runoff graph has a higher MSE value than the other two output variables from the first epoch to the end. The sediment yield regression loss is almost always less than the other two and after epoch 150 (The third decay of the learning rate) it suddenly diverges from them. As a result, the runoff and the soil loss ends at almost the same value (about -12.5 in the log scale), while the sediment yield finishes at a lower point (about -13 in the log scale). It means that the third step of the learning rate decay has a higher impact on the weights and the biases between the FC layer of size 16 and the FC layer of size 1 with the Sigmoid activation function in part B of the Emulator. Finally, the runoff and the soil loss converge as they reach the final epochs. It shows that at some point, the soil loss graph does not significantly decrease so the runoff graph is able to catch it.

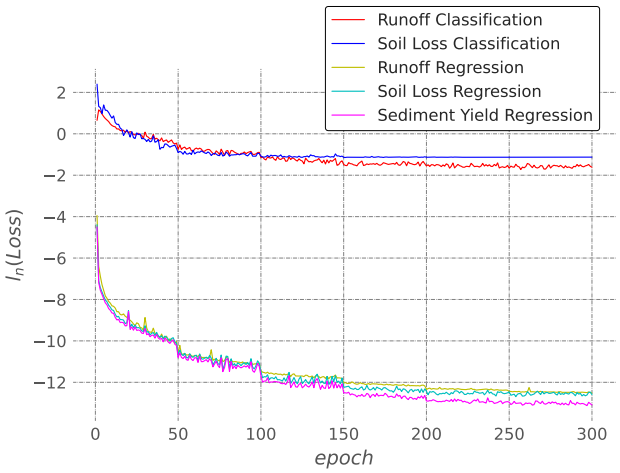

Figure 2. The graphs of the training loss of the five Emulator outputs. We used the natural logarithms (l_n) of the loss values to better demonstrate the changes and the differences.

4.3 The Accuracy of the Emulator

Figure (3) demonstrates the scatter plots of the RHEM outputs versus the Emulator outputs for the merged test dataset (10-fold cross validation) along with the best-fit lines. The slopes of the fitted lines are equal to 1 or very close (statistically significant at 0.001 level), and the intercept values are close to zero in all cases. Also the NSE value of the runoff is 1.0 and 0.999 for the other two output variables (soil loss and sediment yield). These numbers show strong relationships between the output values of the two models. The α for the runoff is 0.994 and for the other two outputs is 1.0. It means that the estimated Emulator outputs and the observed RHEM outputs have almost the same variability. The β for the runoff is 0.004, and for the soil loss and the sediment yield is 0.0. These numbers exhibit that there is no significant bias in the Emulator estimations of the RHEM outputs.

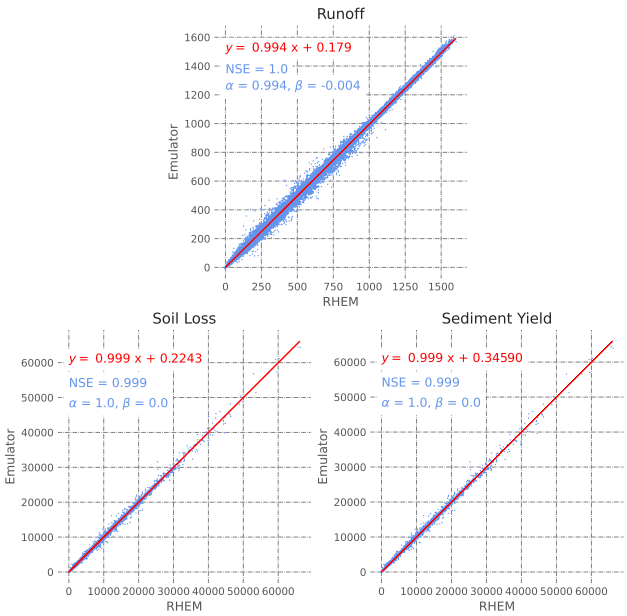

Figure 3. The RHEM outputs versus the Emulator outputs from the 10-fold cross validation. The equations in red show the details of the fitted lines and the NSE, α and β values in blue are the measures described in section 2.3

The classifiers of the Emulator are not based on separate layers and they are just two binarization functions that help the model to generate roughly zero-value predictions (i.e., no runoff or soil loss). The classification accuracy metrics demonstrate the value of including such functions in the regression model. The precision, recall and the F1-score of the runoff classifier in predicting the zero values are 97%, 99% and 98% respectively. These values for non-zero predictions are 99.9%. Thus, using runoff classifier, 99% of the zero cases and 99.9% of the non-zero cases were predicted correctly. Also, 97% of all the zero predictions were correct. The average runoff values of the cases that the runoff classifier incorrectly predicted zero is 5.67×10^{-6}. On the other hand, the average predicted runoff values of the cases that the classifier incorrectly predicted non-zero is 1.66×10^{-6}. These numbers show that adding a runoff classifier to the Emulator (which does not add any extra parameters) is helpful in refining the runoff estimation, while not harming the regression accuracy. The precision, recall and the F1-score of the soil loss classifier in predicting the zero values are 44%, 99.9% and 61% respectively. These values for non-zero predictions are 99.9%, 98%, 99%. The soil loss classifier gets 99.9% of the zero cases and 98% of the non-zero cases correct. Also, 44% of all the zero predictions were correct, meaning that the model tends to predict non-zeros more than zeros – however, the average predicted soil loss values of the cases that the classifier incorrectly predicted non-zero is 3.15×10^{-8}, which means that this misclassification does not significantly harm the soil loss and sediment yield regressions. Moreover, the average soil loss values in the cases where the classifier incorrectly predicted zero is 1.58×10^{-5}, which is very small and likely due to numerical artifacts in RHEM. This also demonstrates that adding an erosion classifier to the Emulator (which also does not add any extra parameters) is marginally helpful in refining the soil loss (and sediment yield) estimation while not harming the regression accuracy.

We trained the Emulator with the whole synthetic dataset and by that we estimated the runoff, soil loss and sediment yield values of the NRI scenarios. Panel (a) of Figure (4) shows the scatter plots of the RHEM outputs versus the Emulator outputs along with

the fitted lines. Comparing the range of the plots in Figure (4) with Figure (3), it can be claimed that the range of the runoff values of the NRI dataset is about half of the range of the synthetic dataset, while the range of the soil loss and sediment yield values in the NRI dataset is a small portion (0.005) of the synthetic range. The Slope of the fitted line, NSE, α, and β are lower than the results of the cross-validation on Figure (3) in all cases. Also, visually inspecting, there are some cases with relatively bad predictions specially within the runoff scatter plot. Panel (b) of Figure 4 demonstrates the scatter plots of the RHEM outputs versus the outputs of the fine-tuned Emulator in a 10-fold cross validation process using the NRI dataset. The accuracy metrics grow in all cases. Also, there are no artifacts in the scatter plots and the points are more concentrated around the fitted lines. In another experiment, instead of fine-tuning the Emulator, we trained the Emulator from scratch with the NRI dataset (we used the same hyperparameters except for the batch size which was reduced to 100 because the NRI data size is less than the synthetic dataset). Panel (c) of Figure 4 shows the result of the 10-fold cross validation of this experiment. In most cases the metrics got worse compared with the fine-tuning results. The NSE of the soil loss and sediment yield drops by more than 15% and the bias of the runoff is three times more. This experiment shows that, in addition to having a comprehensive Emulator, fine-tuning the base model gives better accuracy compared with training the model from scratch with the NRI data only.

4.4 Sensitivity Analysis

Figure (5) shows the first order effects of the FAST GSA for both RHEM and the Emulator over the merged test dataset of the 10-fold cross validation (Section 2.4). We did not include the detailed foliar and ground cover categories in the GSA because one of the assumptions of variance-based GSA is the independence of the parameters. The sensitivity of both models are similar, with only small differences in each parameter. The runoff is mostly controlled by the soil and the climate parameters – Wei et al. (2007) showed a similar effect for event-based RHEM simulations using a local sensitivity analysis. Figure (5) also shows that for all inputs except slope shape, sediment yield is less sensitive to inputs than soil loss. Moreover, the most important factors for soil erosion outputs are slope and ground cover. In contrast, Wei et al. (2007) showed that the most determinant factor of soil loss is total precipitation (prcp) and precipitation duration (dur). This discrepancy may come from the differences in the formulations of the fundamental equation to estimate soil erosion; Wei et al. (2007) used a steady-state approach while, here we used a fully dynamic system of the RHEM version 2.4 (Equation 2). In addition, Wei et al. (2007) used a shear stress sediment formulation but, RHEM version 2.4 uses a stream power formulation. Finally, Wei et al. (2007) derived different parameter estimation equations to estimate hydraulic conductivity, interill, and rill soil erosion. It is also important to note that Wei et al. (2007) used the individual storm events for their sensitivity analysis while, here, we used the annual average values and this may have also played a role in the aforementioned discrepancy.

Among the climatic inputs, both models are more sensitive to the time to rainfall peak (tp) – meaning that, the time to the peak of a storm event is more important than total rainfall or storm duration for average outputs in the long term. Longer time to peak means that there is more time for infiltration, which leads to less runoff and less erosion. Finally, the lower importance of foliar cover compared with ground cover for both models indicates that the flow velocity reduction role of the Ground cover is more important than the rainfall energy weakening role of the foliar cover (Simanton et al., 1991; McCool et al., 2004).

4.5 Change in the Model Prediction by Altering the Variables

Figure 6 demonstrates the graphs of the changes in the Emulator outputs versus the RHEM outputs when each input to the RHEM web application (Table 1) is altered.

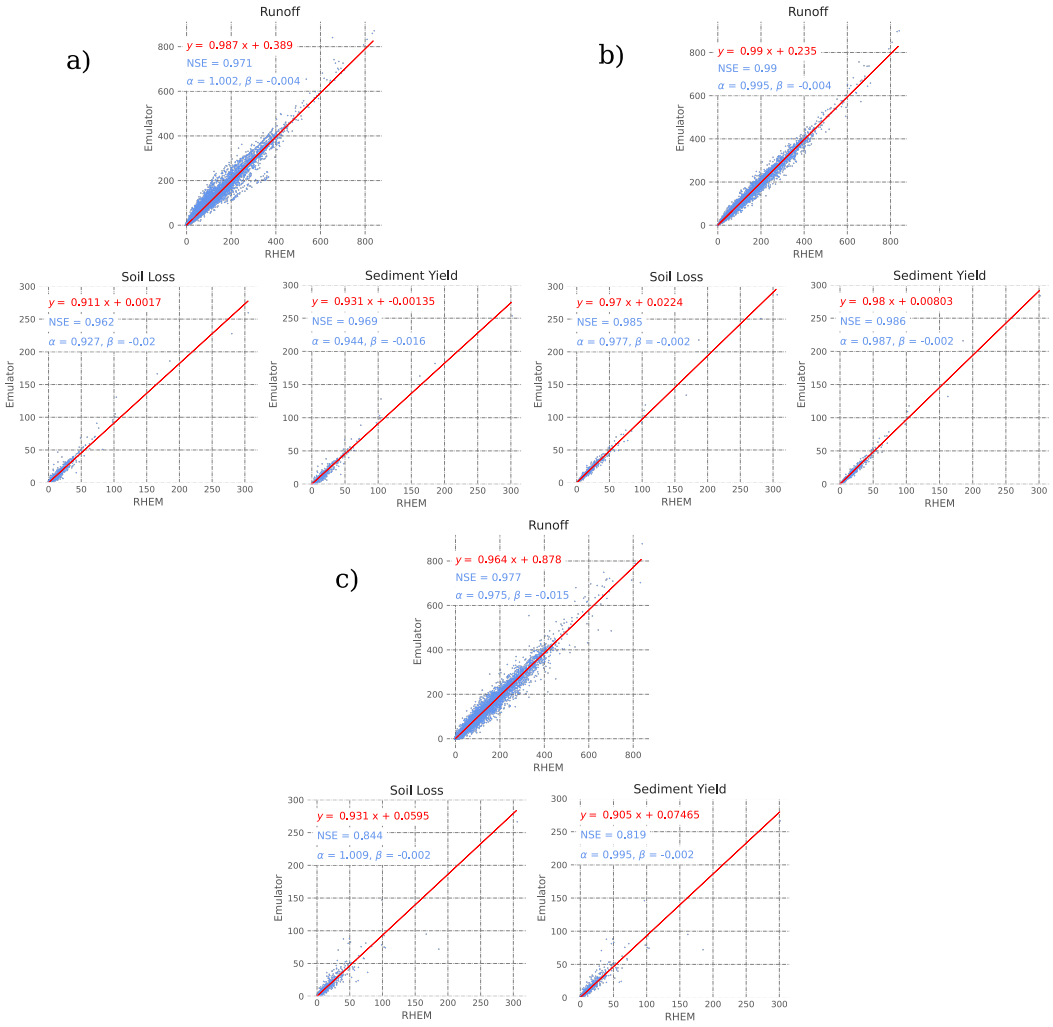

Figure 4. The RHEM outputs versus the Emulator outputs for the NRI dataset of size 32,426 samples: a) Before fine tuning the Emulator, b) After fine tuning the Emulator with the NRI dataset (10-fold cross validation) and, c) Train the Emulator from scratch by NRI data only (10-fold cross validation)

According to Figure 6, the change pattern of the Emulator is similar to the RHEM for all of the variables and outputs and the Emulator can effectively capture all of the changes in the outputs when the variables vary. There are some small divergences between the two graphs in the slope, CLIGEN and the soil plots: When the slope is extremely high (more than 85%), the Emulator overestimates the soil loss and the sediment yield; the V-shaped graphs can be seen in all of the Slope shape panels and the only part that the graphs do not overlap is for the Concave shape of the soil loss panel. for the moderate storm duration (dur) and high time to peak (tp) values the Emulator underestimates the soil loss and the sediment yield; for the cases that we change the soil type to the "Sandy Clay" the Emulator overestimates the soil loss and the sediment yield, while for "Sandy Loam" the opposite is true.

The graphs of Figure 6 are compatible with the results of the GSA (Figure 5) as expected. One extra noteworthy point that can be extracted from Figure 6 is the effect of each Foliar and Ground cover categories. According to the GSA, the runoff is slightly

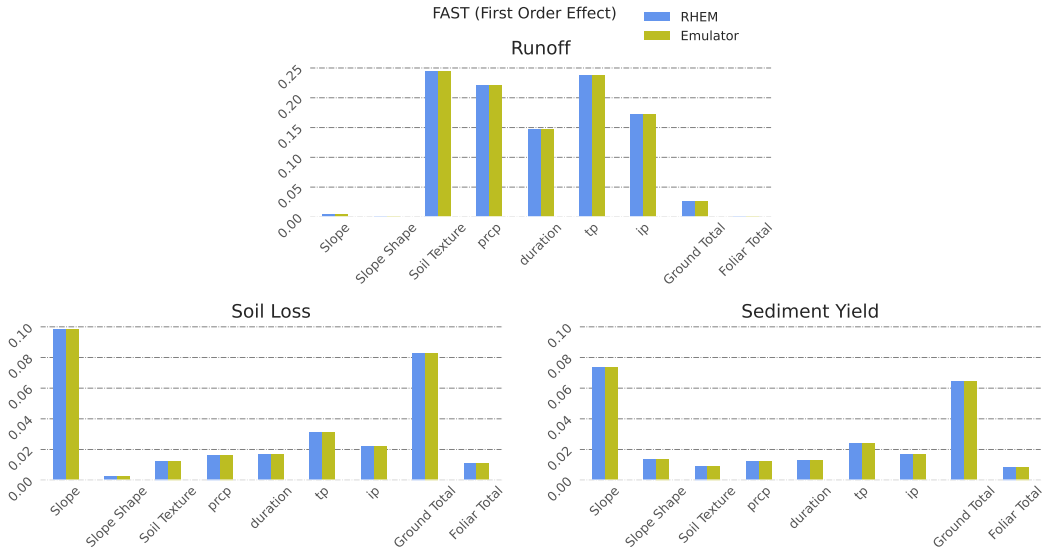

Figure 5. The first order effects of the FAST sensitivity analysis for the RHEM and the Emulator.

sensitive to the ground cover and based on Figure 6, it can be claimed that the Basal and the Litter covers are responsible for that sensitivity level. The reason is that, the Basal and the Litter cover values are directly utilized in estimating the K_e and f in Equation (1) while the other two categories are used secondarily (Hernandez et al., 2017). Also, all the categories are equally responsible for the effect of the Ground and Foliar cover on the soil loss and the sediment yield.

4.6 Dynamic Prediction Behaviors of the Models

Figure 7 shows the statistical tests of comparing the dynamic prediction behaviors of the RHEM versus the Emulator. The left panel exhibits the histogram of the difference between the RHEM outputs of two timestamps (t1 and t2). We extracted the outliers of the difference values and then we fit the normal distributions to the remaining values. We divided the difference values into seven categories based on the distances to the means of the distributions and colored them for easier visualization. The middle panel shows the results of the Pearson's correlation test between the difference values calculated by the RHEM and the difference values calculated by the Emulator for each colored category. Also, the right panel demonstrates the results of the independent t-test between the mean value of the differences calculated by the RHEM and the Emulator for each colored category. According to Figure 7, with 95% confidence, we can reject the null hypothesis of no linear relationships between the difference values in all categories of the three outputs except for the runoff's category of the values less than two standard deviations from the mean. Also, with 95% confidence, we cannot reject the null hypothesis of having equal averages in all categories of the three outputs.

Implementing the tests on the entire difference values without the categorization shows that: For the runoff, the t-test value is equal to -0.146 with the P value of 0.88 which means that the average of the difference values for the Emulator is statistically equal to the RHEM with 95% confidence. The Pearson's correlation values is equal to 0.99 with the P value of almost 0.0 which shows that the direction of the changes in the difference values for the Emulator is statistically similar to the RHEM with 95% confidence. The same tests for the soil loss and the sediment yield exhibit the same rela-

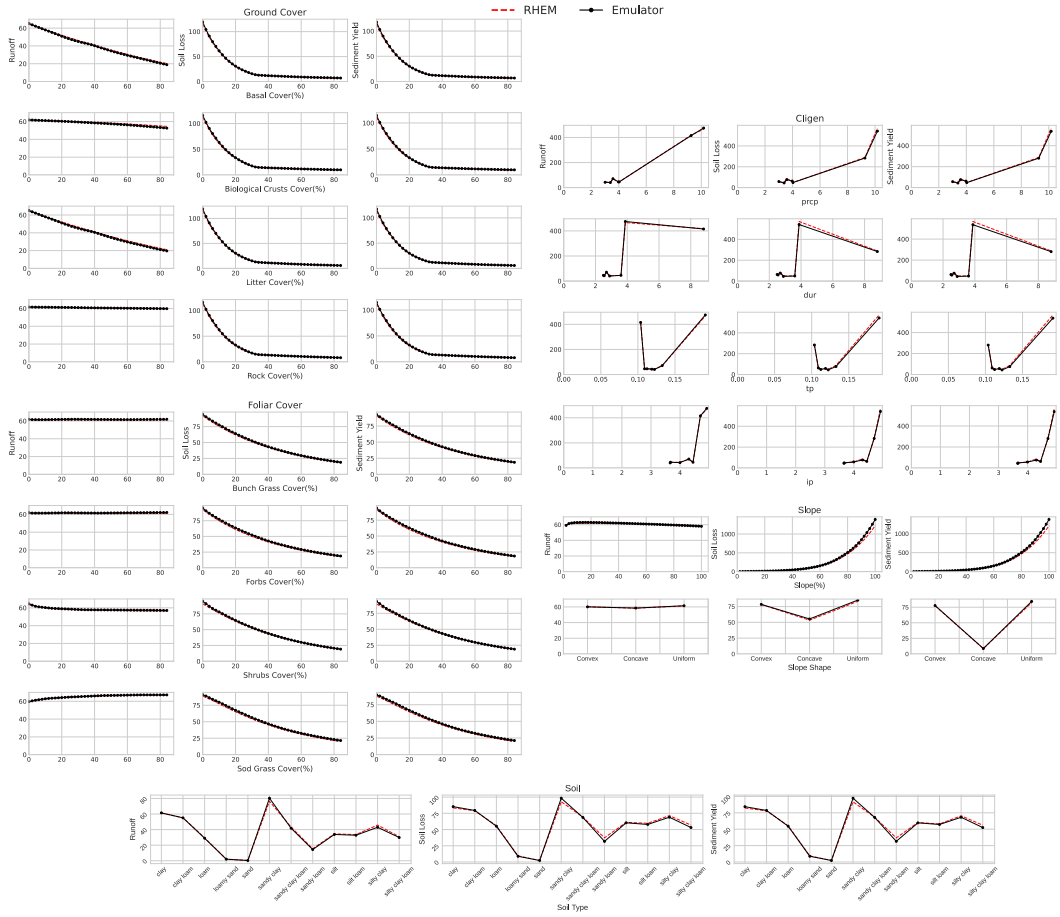

Figure 6. Change pattern of the Emulator outputs versus the RHEM outputs when a variable is altered and the others are fixed.

tionships: For the soil loss, the t-test value is -0.046 (P value: 0.96) and the Pearson's correlation value is 0.99 (P Value: 0.0); For the sediment yield, the t-test value is -0.194 (P value: 0.85) and the Pearson's correlation value is 0.99 (P Value: 0.0). Based on these numbers we can claim that, overall, the dynamic prediction behavior of the Emulator is similar to the RHEM. In other words, in a dynamic landscape, a change in the prediction of the Emulator from time t_1 to time t_2 is similar to the RHEM.

5 Conclusions

The process-based models have been widely used to understand and simulate the systems of the Earth and to predict the future scenarios. The RHEM is one of those models which requires solving two PDEs for more than 100,000 times on each run (It takes about 8 minutes on average). This imposes a prohibitive computational demand. Consequently, the tasks in which we need an enormous amount of model runs, such as sensitivity analysis of the model or making the regional and national maps of the soil erosion, would be computationally intensive and requires high performance computing resources. Moreover, when the infiltration parameters are close to their upper bounds, RHEM may not be able to solve the PDEs. To address the above drawbacks, we introduced a regression based surrogate for the RHEM using Artificial Neural Networks. The trained Emulator is able to reproduce the outputs 13 billion times faster than the average time

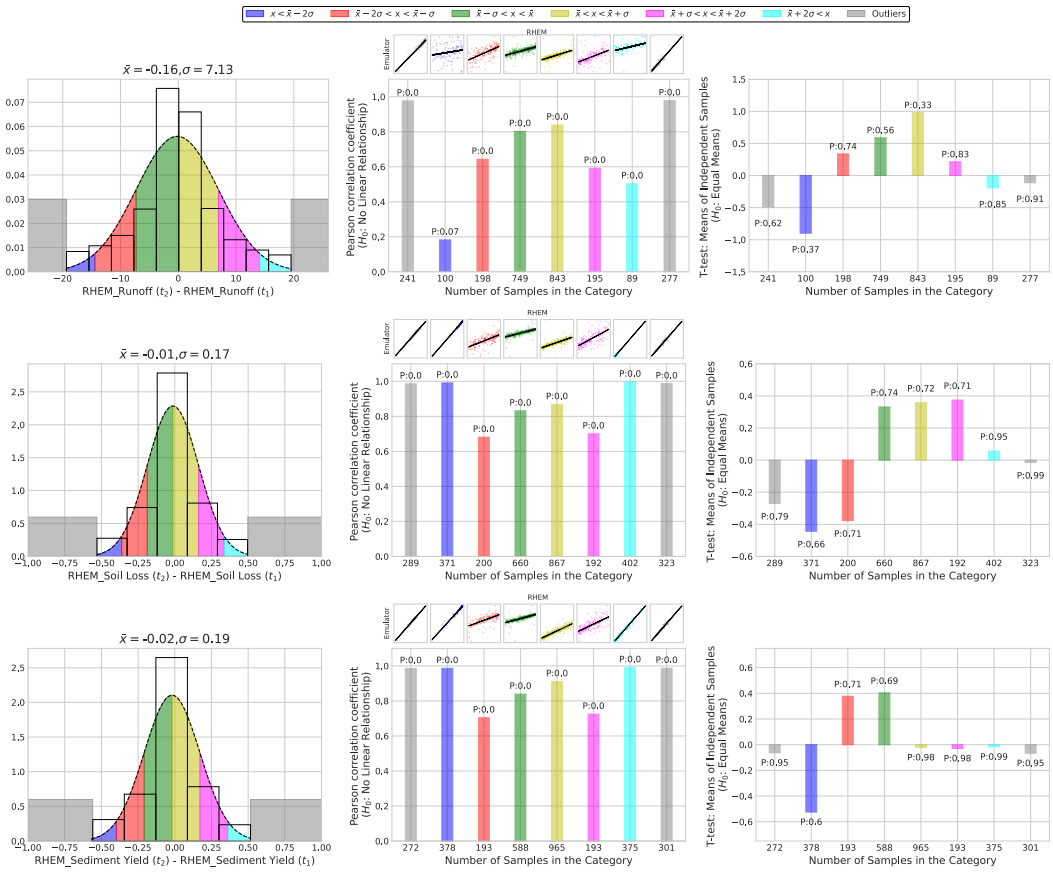

Figure 7. The statistical tests to evaluate the similarity of the dynamic prediction behaviors of the RHEM and the Emulator. The left panel shows the histograms of the samples along with the fitted normal distributions and the outliers. Each color shows a category of the samples. The middle panel demonstrates the results of the Pearson's r correlation test between the values of the RHEM and the Emulator in each category (the small scatter plots on the top visualize the linear relationships). The right panel shows the results of the independent samples t test to compare the averages of the RHEM and the Emulator in each category.

of a RHEM run. For some cases, a RHEM run could take about 41 minutes while the Emulator does not need more than 0.000036 seconds to reproduce the outputs for any case. The Emulator directly calculates the average annual runoff and erosion values while the RHEM needs to calculate the outputs for all of the daily storm events over the 300 years to provide the average values. Finally, there is no scenario in which the Emulator could not be able to provide the outputs even with the extreme infiltration parameters.

We have shown that the proposed Emulator is able to reproduce the RHEM outputs with more that 99% of accuracy for synthetic dataset and with more than 92% of accuracy for the real world dataset. Also, the sensitivity of the Emulator to the input parameters and its dynamic prediction behavior across changing landscapes are similar to the RHEM.

Our approach in this study could be extended in different ways: Recently, solving PDEs by Neural Networks have been introduced as a faster and more robust alternative (Blechschmidt & Ernst, 2021). Our proposed Emulator only uses FC layers (Dense layers) to reproduce a dynamic Physics-based model. One extension to our work is using

the Neural PDE potential to create a network with a similar RHEM architecture that works a lot faster. Another extension to our work is to fine tune the Emulator with the field measured runoff and erosion datasets (e.g. the erosion database collected by Interagency Rangeland Water Erosion Team (Wei et al., 2009)). Since the size of the field measured database is not big enough to train the Emulator from scratch, the weights of the pre-trained network as the prior knowledge could be modified according to the field data to create a posterior model that is able to estimate the real world runoff and erosion values more precisely.

Appendix A Hyperparameter Tuning of the Emulator

The hyperparameters of the model have been tuned using the Bayesian optimization algorithm with Gaussian process (Victoria & Maragatham, 2021). First, we divided the dataset into three subsets: 90% as the training set and, 10% as the test set. Then, for each hyperparameter, we defined some candidates for its optimum value. Table A1 shows the list of hyperparameters and their optimum candidates. The Bayesian algorithm starts with a random scenario among all possible combinations of the hyperparameters and trains the model by that using the training set for 300 epochs. It then evaluates the trained model using the test set (The training process stopped if after 10 consecutive epochs the validation metrics did not change). Considering the validation error, the algorithm chooses the next scenario. That is, the algorithm takes into account the history of hyperparameter scenarios for choosing the next one until it reaches a minimum. Equation (A1) shows the error function for the validation:

$$e_{obj} = \frac{\frac{\sqrt{\frac{\sum_{i=1}^{N}(x_i-\hat{x}_i)^2}{N}}}{x_{max}-x_{min}} + \frac{\sqrt{\frac{\sum_{i=1}^{N}(y_i-\hat{y}_i)^2}{N}}}{y_{max}-y_{min}} + \frac{\sqrt{\frac{\sum_{i=1}^{N}(z_i-\hat{z}_i)^2}{N}}}{z_{max}-z_{min}}}{3} \tag{A1}$$

where e_{obj} is the objective error function. x_i is the runoff from the RHEM and $\hat{x_i}$ is the predicted runoff from the trained Emulator. $x_{min}-x_{max}$ is the range of the runoff values from the RHEM. y_i is the soil loss from the RHEM and $\hat{y_i}$ is the predicted soil loss from the trained Emulator. $y_{min}-y_{max}$ is the range of the soil loss values from the RHEM. Also, z_i is the sediment yield from the RHEM, and $\hat{z_i}$ is the predicted sediment yield from the trained Emulator. $z_{min}-z_{max}$ is the range of the sediment yield values from the RHEM. The function is basically the average of the normalized root mean square errors of the runoff, soil loss, and sediment yield.

Table A1. The Hyperparameters of the Emulator and their possible optimum values.

Hyperparameter	Values
Dense layer Size1	[64, 128, 256, 512]
Dense layer Size2	[16, 32, 64]
Initial Learning Rate	[0.01, 0.001, 0.0001]
Learning Rate Scheduler-Parameter1	[0.1, 0.5, 0.9]
Learning Rate Scheduler-Parameter2	[10, 25, 50, 100]
Batch Size	[100, 500, 1000, 2000]

The algorithm reached [512,16,0.0001,0.9,10,2000] on trial 37 and did not change after that. Figure A1 depicts the 20 trials with the lowest objective error values along with the details of the first 3. The more thick and dark a curve is, the less its objective error. Based on Figure A1, The model with the lowest error (we call it trial 1) has 2,667,141 trainable parameters while the model is based on the second-lowest error (we call it trial

2) has 678,277 trainable parameters. The Dense layer Size2 for both trials is 16. The learning rate for trial 2 is small at first and it slightly decreases after every 25 epochs. The learning rate of trial 2 starts from a larger value and it decreases slightly and more frequently (every 10 epochs). The batch size of trial 1 is four times bigger than trial 2 which means it has fewer changes in the model parameters during an epoch. To sum up, trial 1 tends to learn with fewer parameter adjustments and bigger steps that do not change that much while trial 2 learns with more modifications of the parameters and smaller step sizes that change more frequently.

The Bayesian algorithm does not guarantee to find the global minimum of the error and the best combination of the hyper parameters and it tries to find the one which is close to the optimum. So, we removed 32 and 64 from the candidates of the Dense layer Size2 and ran the Bayesian algorithm again. This time it reaches [256,16,0.0001,0.9,10,500] on trial 29 and did not change after that. The minimum error for this scenario is 0.00321 which is less than the best trial in Figure (A1). We then only kept the 256 for Dense layer Size1 and conducted the algorithm for the third time. This time it reached [256,16,0.001,0.5,50,500] after trial 22. The minimum error for this scenario is 0.00256. Finally, we manually tried other combinations of the learning rate parameters and the batch size to reduce the error function even more. We realized that by increasing the batch size up to 1,000 the error drops to 0.00186. Thus we decided to use [256,16,0.001,0.5,50,1000] as the hyper-parameters of the Emulator.

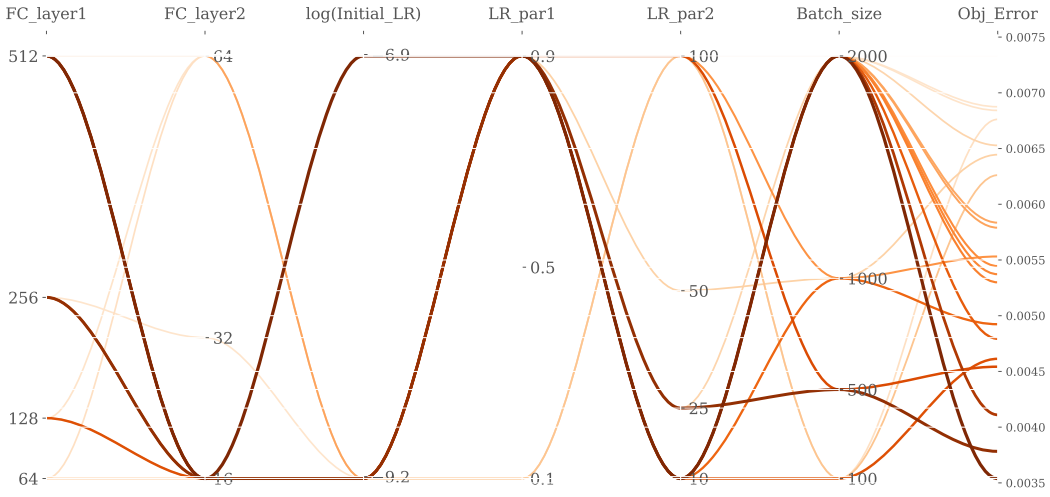

	FC_layer1	FC_layer2	Initial_LR	LR_par1	LR_par2	Batch_size	Obj_error
1	512	16	0.001	0.9	10	2000	0.00354
2	256	16	0.0001	0.9	25	500	0.00378
3	512	16	0.0001	0.9	10	2000	0.00410

Figure A1. The parallel coordinate plot of the hyper parameter tuning of the Emulator. The more thick and dark a curve is, the less its objective error. The table shows the details of the three best trials.

Data Availability Statement

The NRI and synthetic RHEM scenarios and outputs as well as the RHEM Emulator, our training pipeline, all of the Python scripts we used for cross validation and sensitivity analysis, and our model's pre-trained weights are open source and publicly available via `https://github.com/saeedimd/RHEM-ML.git` (DOI: 10.5281/zenodo.6599824)

Acknowledgments

This material is based upon work supported by the U.S. Department of Agriculture, Natural Resources Conservation Service, Conservation Effects Assessment Project (CEAP) Grazing Lands Component, under agreement number NR193A750007C002. Any opinions, findings, conclusions, or recommendations expressed in this publication are those of the author(s) and do not necessarily reflect the views of the U.S. Department of Agriculture. In addition, any reference to specific brands or types of products or services does not constitute or imply an endorsement by the U.S. Department of Agriculture for those products or services.

References

Abadi, M., Agarwal, A., Barham, P., Brevdo, E., Chen, Z., Citro, C., ... Zheng, X. (2015). *TensorFlow: Large-scale machine learning on heterogeneous systems.* Retrieved from `https://www.tensorflow.org/` (Software available from tensorflow.org)

Al-Hamdan, O. Z., Hernandez, M., Pierson, F. B., Nearing, M. A., Williams, C. J., Stone, J. J., ... Weltz, M. A. (2015). Rangeland hydrology and erosion model (rhem) enhancements for applications on disturbed rangelands. *Hydrological Processes*, *29*(3), 445-457. Retrieved from `https://onlinelibrary.wiley.com/doi/abs/10.1002/hyp.10167` doi: https://doi.org/10.1002/hyp.10167

A. Nearing, M., Foster, G., Lane, L., & Finkner, S. (1989). A process-based soil erosion model for usda-water erosion prediction project technology. *Transactions of the ASAE*, *32*(5), 1587–1593.

Aurelio, Y. S., de Almeida, G. M., de Castro, C. L., & Braga, A. P. (2019, October). Learning from imbalanced data sets with weighted Cross-Entropy function. *Neural Processing Letters*, *50*(2), 1937–1949.

A. Weltz, M., Jolley, L., Hernandez, M., E. Spaeth, K., Rossi, C., Talbot, C., ... Morris, C. (2014). Estimating conservation needs for rangelands using usda national resources inventory assessments. *Transactions of the ASABE*, *57*(6), 1559-1570. Retrieved from `https://elibrary.asabe.org/abstract.asp?aid=45283&t=3`

Blechschmidt, J., & Ernst, O. G. (2021). Three ways to solve partial differential equations with neural networks — a review. *GAMM-Mitteilungen*, *44*(2), e202100006. Retrieved from `https://onlinelibrary.wiley.com/doi/abs/10.1002/gamm.202100006` doi: https://doi.org/10.1002/gamm.202100006

Cruse, R., Flanagan, D., Frankenberger, J., Gelder, B., Herzmann, D., James, D., ... Todey, D. (2006). Daily estimates of rainfall, water runoff, and soil erosion in iowa. *Journal of Soil and Water Conservation*, *61*(4), 191–199. Retrieved from `https://www.jswconline.org/content/61/4/191`

Cukier, R. I., Fortuin, C. M., Shuler, K. E., Petschek, A. G., & Schaibly, J. H. (1973). Study of the sensitivity of coupled reaction systems to uncertainties in rate coefficients. i theory. *The Journal of Chemical Physics*, *59*(8), 3873-3878. Retrieved from `https://doi.org/10.1063/1.1680571` doi: 10.1063/1.1680571

Dooge, J. C. I. (1986). Looking for hydrologic laws. *Water Resources Research*, *22*(9S), 46S-58S. Retrieved from `https://agupubs.onlinelibrary.wiley.com/doi/abs/10.1029/WR022i09Sp0046S` doi: https://doi.org/10.1029/WR022i09Sp0046S

Gelder, B., Sklenar, T., James, D., Herzmann, D., Cruse, R., Gesch, K., & Laflen, J. (2018). The daily erosion project – daily estimates of water runoff, soil detachment, and erosion. *Earth Surface Processes and Landforms*, *43*(5), 1105-1117. Retrieved from `https://onlinelibrary.wiley.com/doi/abs/10.1002/esp.4286` doi: https://doi.org/10.1002/esp.4286

Gupta, H. V., Kling, H., Yilmaz, K. K., & Martinez, G. F. (2009). Decomposition of the mean squared error and nse performance criteria: Implications for improving hydrological modelling. *Journal of Hydrology*, *377*(1), 80-91. Retrieved from https://www.sciencedirect.com/science/article/pii/S0022169409004843 doi: https://doi.org/10.1016/j.jhydrol.2009.08.003

He, K., Zhang, X., Ren, S., & Sun, J. (2015, dec). Delving deep into rectifiers: Surpassing human-level performance on imagenet classification. In *2015 ieee international conference on computer vision (iccv)* (p. 1026-1034). Los Alamitos, CA, USA: IEEE Computer Society. Retrieved from https://doi.ieeecomputersociety.org/10.1109/ICCV.2015.123 doi: 10.1109/ICCV.2015.123

Herman, J., & Usher, W. (2017). Salib: An open-source python library for sensitivity analysis. *Journal of Open Source Software*, *2*(9), 97. Retrieved from https://doi.org/10.21105/joss.00097 doi: 10.21105/joss.00097

Hernandez, M., Nearing, M. A., Al-Hamdan, O. Z., Pierson, F. B., Armendariz, G., Weltz, M. A., ... Holifield Collins, C. D. (2017). The rangeland hydrology and erosion model: A dynamic approach for predicting soil loss on rangelands. *Water Resources Research*, *53*(11), 9368-9391. Retrieved from https://agupubs.onlinelibrary.wiley.com/doi/abs/10.1002/2017WR020651 doi: https://doi.org/10.1002/2017WR020651

Hsu, K.-l., Gupta, H. V., Gao, X., Sorooshian, S., & Imam, B. (2002). Self-organizing linear output map (solo): An artificial neural network suitable for hydrologic modeling and analysis. *Water Resources Research*, *38*(12), 38-1-38-17. Retrieved from https://agupubs.onlinelibrary.wiley.com/doi/abs/10.1029/2001WR000795 doi: https://doi.org/10.1029/2001WR000795

Ioffe, S., & Szegedy, C. (2015, 07–09 Jul). Batch normalization: Accelerating deep network training by reducing internal covariate shift. In F. Bach & D. Blei (Eds.), *Proceedings of the 32nd international conference on machine learning* (Vol. 37, pp. 448–456). Lille, France: PMLR. Retrieved from http://proceedings.mlr.press/v37/ioffe15.html

Kingma, D. P., & Ba, J. (2014, December). Adam: A Method for Stochastic Optimization. *arXiv e-prints*.

Kratzert, F., Klotz, D., Herrnegger, M., Sampson, A. K., Hochreiter, S., & Nearing, G. S. (2019). Toward improved predictions in ungauged basins: Exploiting the power of machine learning. *Water Resources Research*, *55*(12), 11344-11354. Retrieved from https://agupubs.onlinelibrary.wiley.com/doi/abs/10.1029/2019WR026065 doi: https://doi.org/10.1029/2019WR026065

Lane, L. J., & Nearing, M. A. (1989). *Usda-water erosion prediction project: Hillslope profile model documentation* (Tech. Rep.). USDA-ARS National Soil Erosion Research Laboratory.

Lange, H., & Sippel, S. (2020). Machine learning applications in hydrology. In D. F. Levia, D. E. Carlyle-Moses, S. Iida, B. Michalzik, K. Nanko, & A. Tischer (Eds.), *Forest-water interactions* (pp. 233–257). Cham: Springer International Publishing. Retrieved from https://doi.org/10.1007/978-3-030-26086-6_10 doi: 10.1007/978-3-030-26086-6_10

McCool, D., Foster, G., & Daniel, Y. (2004). The revised universal soil loss equation, version 2. In *13th international soil conservation organization conference* (p. 4–8,). Brisbane, Australia.

Mckay, M. D., Beckman, R. J., & Conover, W. J. (2000). A comparison of three methods for selecting values of input variables in the analysis of output from a computer code. *Technometrics*, *42*(1), 55-61. Retrieved from https://www.tandfonline.com/doi/abs/10.1080/00401706.2000.10485979 doi: 10.1080/00401706.2000.10485979

Mohammadi, S., & Cremaschi, S. (2019). Efficiency of uncertainty propagation methods for estimating output moments. In S. G. Muñoz, C. D. Laird,

& M. J. Realff (Eds.), *Proceedings of the 9th international conference on foundations of computer-aided process design* (Vol. 47, p. 487-492). Elsevier. Retrieved from https://www.sciencedirect.com/science/article/pii/B9780128185971500783 doi: https://doi.org/10.1016/B978-0-12-818597-1.50078-3

Nearing, G. S., Kratzert, F., Sampson, A. K., Pelissier, C. S., Klotz, D., Frame, J. M., ... Gupta, H. V. (2021). What role does hydrological science play in the age of machine learning? *Water Resources Research*, *57*(3), e2020WR028091. Retrieved from https://agupubs.onlinelibrary.wiley.com/doi/abs/10.1029/2020WR028091 (e2020WR028091 10.1029/2020WR028091) doi: https://doi.org/10.1029/2020WR028091

Nearing, G. S., Ruddell, B. L., Clark, M. P., Nijssen, B., & Peters-Lidard, C. (2018). Benchmarking and process diagnostics of land models. *Journal of Hydrometeorology*, *19*(11), 1835 - 1852. Retrieved from https://journals.ametsoc.org/view/journals/hydr/19/11/jhm-d-17-0209_1.xml doi: 10.1175/JHM-D-17-0209.1

Renda, A., Frankle, J., & Carbin, M. (2020). Comparing rewinding and fine-tuning in neural network pruning. In *International conference on learning representations.* Retrieved from https://openreview.net/forum?id=S1gSj0NKvB

Saltelli, A., Annoni, P., Azzini, I., Campolongo, F., Ratto, M., & Tarantola, S. (2010). Variance based sensitivity analysis of model output. design and estimator for the total sensitivity index. *Computer Physics Communications*, *181*(2), 259-270. Retrieved from https://www.sciencedirect.com/science/article/pii/S0010465509003087 doi: https://doi.org/10.1016/j.cpc.2009.09.018

Santurkar, S., Tsipras, D., Ilyas, A., & Madry, A. (2018). *How does batch normalization help optimization?* arXiv. Retrieved from https://arxiv.org/abs/1805.11604 doi: 10.48550/ARXIV.1805.11604

Satterthwaite, F. E. (1959). Random balance experimentation. *Technometrics*, *1*(2), 111-137. Retrieved from https://www.tandfonline.com/doi/abs/10.1080/00401706.1959.10489853 doi: 10.1080/00401706.1959.10489853

Simanton, J. R., Weltz, M. A., & Larsen, H. D. (1991). Rangeland experiments to parameterize the water erosion prediction project model: Vegetation canopy cover effects. *Journal of Range Management*, *44*(3), 276–282. Retrieved from http://www.jstor.org/stable/4002957

Sit, M., Demiray, B. Z., Xiang, Z., Ewing, G. J., Sermet, Y., & Demir, I. (2020, 08). A comprehensive review of deep learning applications in hydrology and water resources. *Water Science and Technology*, *82*(12), 2635-2670. Retrieved from https://doi.org/10.2166/wst.2020.369 doi: 10.2166/wst.2020.369

Soil Survey Staff, S. C. S. (1999). *Soil taxonomy: A basic system of soil classification for making and interpreting soil surveys* (2nd ed.). Natural Resources Conservation Service. U.S. Department of Agriculture. Retrieved from https://www.nrcs.usda.gov/Internet/FSE_DOCUMENTS/nrcs142p2_051232.pdf

Sun, C., Shrivastava, A., Singh, S., & Gupta, A. (2017, oct). Revisiting unreasonable effectiveness of data in deep learning era. In *2017 ieee international conference on computer vision (iccv)* (p. 843-852). Los Alamitos, CA, USA: IEEE Computer Society. Retrieved from https://doi.ieeecomputersociety.org/10.1109/ICCV.2017.97 doi: 10.1109/ICCV.2017.97

Tajbakhsh, N., Shin, J. Y., Gurudu, S. R., Hurst, R. T., Kendall, C. B., Gotway, M. B., & Liang, J. (2016, May). Convolutional neural networks for medical image analysis: Full training or fine tuning? *IEEE Transactions on Medical Imaging*, *35*(5), 1299-1312. doi: 10.1109/TMI.2016.2535302

Tarantola, S., Gatelli, D., & Mara, T. (2006). Random balance designs for the estimation of first order global sensitivity indices. *Reliability En-*

gineering & System Safety, *91*(6), 717-727. Retrieved from https://www.sciencedirect.com/science/article/pii/S0951832005001444 doi: https://doi.org/10.1016/j.ress.2005.06.003

USDA, N. R. C. S. (2018). *National resources inventory: Grazing land onsite data study, 2004-2018 data provided by usda nrcs for purposes of this project, https://www.nrcs.usda.gov/wps/portal/nrcs/main/national/technical/nra/nri/.*

US Department of Agriculture, N. R. C. S. (2019). National resources inventory grazing land on-site data collection handbook of instructions.

Victoria, A. H., & Maragatham, G. (2021, Mar 01). Automatic tuning of hyperparameters using bayesian optimization. *Evolving Systems*, *12*(1), 217-223. Retrieved from https://doi.org/10.1007/s12530-020-09345-2 doi: 10.1007/s12530-020-09345-2

Vrbančič, G., & Podgorelec, V. (2020). Transfer learning with adaptive fine-tuning. *IEEE Access*, *8*, 196197-196211. doi: 10.1109/ACCESS.2020.3034343

Wang, Y., Yao, Q., Kwok, J. T., & Ni, L. M. (2020, jun). Generalizing from a few examples: A survey on few-shot learning. *ACM Comput. Surv.*, *53*(3). Retrieved from https://doi.org/10.1145/3386252 doi: 10.1145/3386252

Wei, H., Nearing, M., Stone, J., Guertin, D., Spaeth, K., Pierson, F., ... Moffet, C. (2009). A new splash and sheet erosion equation for rangelands. *Soil Science Society of America Journal*, *73*(4), 1386-1392. Retrieved from https://acsess.onlinelibrary.wiley.com/doi/abs/10.2136/sssaj2008.0061 doi: https://doi.org/10.2136/sssaj2008.0061

Wei, H., Nearing, M. A., & J. Stone, J. (2007). A comprehensive sensitivity analysis framework for model evaluation and improvement using a case study of the rangeland hydrology and erosion model. *Transactions of the ASABE*, *50*(3), 945-953. Retrieved from https://elibrary.asabe.org/abstract.asp?aid=23159&t=3

Xu, C., & Gertner, G. (2011). Understanding and comparisons of different sampling approaches for the fourier amplitudes sensitivity test (fast). *Computational Statistics & Data Analysis*, *55*(1), 184-198. Retrieved from https://www.sciencedirect.com/science/article/pii/S0167947310002756 doi: https://doi.org/10.1016/j.csda.2010.06.028

Zhuang, F., Qi, Z., Duan, K., Xi, D., Zhu, Y., Zhu, H., ... He, Q. (2021). A comprehensive survey on transfer learning. *Proceedings of the IEEE*, *109*(1), 43-76. doi: 10.1109/JPROC.2020.3004555